TOPICS
TOPICS IN COGNITIVE SCIENCE

Topics in Cognitive Science 00 (2023) 1–18

ISSN: 1756-8765 online
DOI: 10.1111/tops.12688

This article is part of the topic "The Dynamical Hypothesis Three Decades Later: Advances, Critiques, and Prospects for a Dynamical Cognitive Science," Luis H. Favela and Vicente Raja (Topic Editors).

A Multivariate Method for Dynamic System Analysis: Multivariate Detrended Fluctuation Analysis Using Generalized Variance

Sebastian Wallot,[a,b] Julien Patrick Irmer,[c] Monika Tschense,[a,d] Nikita Kuznetsov,[e] Andreas Højlund,[b,f,g] Martin Dietz[g]

[a] *Institute for Sustainability Education and Psychology, Leuphana University of Lüneburg*
[b] *Interacting Minds Centre, Aarhus University*
[c] *Department of Psychology, Goethe University of Frankfurt*
[d] *Research Group for Neurocognition of Music and Language, Max Planck Institute for Empirical Aesthetics*
[e] *Department of Rehabilitation, Exercise, and Nutrition Sciences, University of Cincinnati*
[f] *Department of Linguistics, Cognitive Science and Semiotics, Aarhus University*
[g] *Center of Functionally Integrative Neuroscience, Department of Clinical Medicine, Aarhus University*

Received 23 March 2023; received in revised form 16 August 2023; accepted 22 August 2023

Abstract

Fractal fluctuations are a core concept for inquiries into human behavior and cognition from a dynamic systems perspective. Here, we present a generalized variance method for multivariate detrended fluctuation analysis (mvDFA). The advantage of this extension is that it can be applied to multivariate time series and considers intercorrelation between these time series when estimating fractal properties. First, we briefly describe how fractal fluctuations have advanced a dynamic system

Sebastian Wallot and Julien Patrick Irmer have contributed equally to the paper and hence share the first authorship.

Correspondence should be sent to Sebastian Wallot, Institute for Sustainability Education and Psychology, Leuphana University of Lüneburg, Universitätsallee 1, 21335 Lüneburg, Germany. E-mail: sebastian.wallot@leuphana.de

understanding of cognition. Then, we describe mvDFA in detail and highlight some of the advantages of the approach for simulated data. Furthermore, we show how mvDFA can be used to investigate empirical multivariate data using electroencephalographic recordings during a time-estimation task. We discuss this methodological development within the framework of interaction-dominant dynamics. Moreover, we outline how the availability of multivariate analyses can inform theoretical developments in the area of dynamic systems in human behavior.

Keywords: Detrended fluctuation analysis; Multivariate analysis; Interaction-dominant dynamics; Time estimation; Dynamic systems; R package

1. Introduction

Whether a question is empirical or metaphysical depends, in part, on methodological developments. Before a tangible theory of atoms with empirical content could be developed, certain technological developments were necessary in order to observe matter and energy at certain scales. The same direction was followed in applications of systems theory—and, in particular, dynamics systems theory—in psychology and cognitive science: System thinking is not new to psychology and is prominently present in the works of eminent scientists such as Lewin (1939), Bronfenbrenner (1976), or Köhler (1940). Just like the theories of atoms of the ancients, these theories had a strong metaphorical character because they lacked a fundamental understanding of dynamic systems and the tools necessary to describe and measure system properties (Favela, 2020) were not available.

Van Gelder (1998) argues that the dynamic hypothesis actually contains two hypotheses: (1) That cognitive agents *are* dynamic systems. (2) That cognitive agents *can be understood* as dynamic systems. Assuming that one tries to understand cognitive agents in terms of dynamic systems, Van Gelder goes on to chart some of the differences between how "dynamicists" view cognition in contrast to "computationalists," who try to understand cognition mainly in terms of computation. Briefly, he summarizes that a dynamic systems perspective on cognition emphasizes a change in time and views the structure of cognition as being the result of the interaction of time-dependent processes, while a computational perspective on cognition emphasizes the presence of stable components that are all present at any moment in time and whose internal complexity is the main source of cognitive activity. In the latter case, complex dynamics observed in a cognitive agent are just the result of the activity of these components, which themselves only interact weakly (Simon, 1973). This set of assumptions about cognition has been called the component-dominant view (Van Orden, Holden, & Turvey, 2003)—the dynamics of a system are dominated by the features of the components that make up the system.

A central problem for the component dominant view is posed by the number of components: As Van Gelder (1998) describes, the number of components needs to be stable and all components need to be always present. As new components are discovered, a better understanding of the cognitive system is reached. Here, interaction effects in basic cognitive tasks pose a challenge: Either they point to the fact that the manipulation at hand did not cleanly target the different cognitive components researchers aim at manipulating (Sternberg,

1969)—or they point to the fact that we need to introduce a new component that can explain the interaction effect (Van Orden, Pennington, & Stone, 2001). However, to the extent that such interaction effects continue to be found in basic cognitive tasks and new components are introduced to explain the results, there may be concern that there is no stable set of components that can be discovered and upon which a computational theory of cognition can be built (Van Orden & Kloos, 2003).

To develop a tangible dynamic systems perspective on this problem and to explain its presence, we remind ourselves of van Gelder's (1998) earlier description of the epistemic dynamic hypothesis: Cognition is not the result of the internal structure of cognitive components but rather the result of interactions of components over time. However, to make a concrete connection between interaction effects in cognitive tasks and the understanding of dynamical systems required the concept of fractal scaling, first observed in human data by Gilden, Thornton, and Mallon (1995) who studied time estimates.

Gilden et al. (1995) had participants perform a repeated timing task, where participants were asked to press a response key repeatedly at a pre-specified time interval. The time series of timing intervals, however, were not uncorrelated but displayed fractal scaling, a.k.a. long memory. Fractal scaling means that there is a relation between two quantities so that one increases (or decreases) as a power-law function of the other (for an introduction to the topic, see Brown & Liebovitch, 2010). In Gilden et al.'s (1995) case, this meant that successive time intervals were not uncorrelated, or only correlated across a few lags (i.e., short memory), but showed long-memory correlations across a wide range of trials, where the decay of these correlations is characterized by a power-law relationship.

Van Orden et al. (2003) realized that this provided an important link of human measurements to properties of self-organization (Van Orden et al., 2003), particularly the concept of self-organized criticality (SOC). SOC is a concept that aims to explain how dynamic systems that are made up of many interacting components can evolve and can exhibit a critical state in which small disturbances or events can trigger large-scale cascades or reactions (Jensen, 1998).

In self-organized critical systems, there is no set of modules that act as a central controller. Rather, such systems are driven by feedback loops between their components, which lead them to naturally settle into a critical state that allows them to be highly responsive—and it has been suggested that SOC is the basic structure of living organisms (Bak, 1996). A crucial aspect of SOC is that its behavior exhibits fractal scaling—the traces of long memory observed by Gilden et al. (1995).

Accordingly, this allowed Van Orden et al. (2003) to interpret interactions in basic cognitive tasks, not as a problem of finding the right components that are the building blocks of cognition, but rather as a consequence of a dynamic system whose components interact over time, and are thus so sensitive to changes in external conditions, such as different experimental setups, as to quickly adapt to such conditions and change their behavior accordingly—yielding new behavior that inferential statistics would recover as interaction effects. Accordingly, this perspective provided an interaction-dominant view of cognition, where it is not the internal structure of cognitive modules, but rather the interactions between them, that dominate cognitive dynamics. In order to make this link, methods that can reliably quantify the strength, type, and complexity of long-memory properties of time series (viz.,

1/*f* noise, fractal fluctuations, flicker noise, or colored noise) were needed—which have since been found in many human behavioral and neurophysiological measures (for reviews, see Kello et al., 2010; Van Orden, Kloos, & Wallot, 2011).

Scaling analyses such as detrended fluctuation analysis (DFA) are at the center of debates about psychological measurement theory (Holden, Choi, Amazeen, & Van Orden, 2011; Kelty-Stephen & Mangalam, 2022) as well as debates on whether and how cognition can be understood as a dynamical system (Kelty-Stephen & Wallot, 2017; Wallot & Kelty-Stephen, 2018; Van Orden et al., 2003; Van Orden, Holden, & Turvey, 2005; Wagenmakers, Farrell, & Ratcliff, 2004, 2005). However, by their very definition, systems are composed of many components; and, conversely, many research designs yield multivariate time series data, for instance, eye tracking, postural sway, motion capture, and electroencephalography (EEG). While univariate fractal scaling has helped to understand cognitive activity from a dynamic systems perspective, it also carries with it the notion that the different components of such systems are interdependent—but the currently available time series analysis methods only allow the quantification of fractal scaling properties for each measured variable separately. To gain new insights into the behavior of whole subsystems, or systems on a global level, combining information from all the measured variables at once might be necessary.

Hence, we present a multivariate extension of the DFA method that estimates long-range correlations of multivariate (i.e., multidimensional) time series. Note that Xiong and Shang (2017) already proposed a multivariate DFA approach for independent time series. Xiong's and Shang's (2017) proposal for a multivariate fractal analysis is thus similar to the total variance method described in this paper. However, we also propose a new, generalized variance method that takes the correlations between the different time series into account. It is an important step because multiple variables measured from the same system are likely to be correlated in most of the cases, and these correlations are not taken into account by Xiong's and Shang's (2017) method.

In the following, we begin by explaining the standard DFA formalism and subsequently derive two multivariate extensions (mvDFA) that capture (mono-)fractal properties of multivariate time series. Both versions are tested on artificial data and EEG data from a timing study and are then compared to the standard formalism. Furthermore, we show how mvDFA can be used to test hypotheses on inherently multivariate datasets. The data can be accessed here: https://osf.io/h2kqb/. Data analyses and implementation of the package mvDFA (Irmer & Wallot, 2023) have been done in R (R Core Team, 2022). Further information about the mvDFA package can be found on GitHub (https://github.com/jpirmer/mvDFA).

2. Detrended fluctuations analysis and its multivariate extensions

The standard DFA function estimates how variance in a time series changes with sample size (Peng, Havlin, Stanley, & Goldberger, 1995). This change is summarized by a scaling exponent H (Hurst exponent) that captures the scaling relation between the length of a time series and the associated variance. If $H = 0.5$, the variance of the time series conforms to white noise (but is not guaranteed to be independently and identically distributed.,

however—e.g., Mandelbrot, 1997). If $H > 0.5$, the time series contains persistent long memory, with variance growing faster over time than expected by the central limit theorem, and potentially nonstationary averages (persistent fluctuations; Holden, 2005). If $H < 0.5$, this is called antipersistent fluctuations. Mathematically, the DFA proceeds in the following steps (see also Fig. 1). First, integrate the time series by cumulative summation of deviations from the mean:

$$y(t) \equiv \sum_{k=1}^{t} [x_k - \bar{x}], \quad t = 1, \cdots, N, \tag{1}$$

where x is the original time series, y is the new time series consisting of the cumulative sum of the centered values of x, N is the length of time series x (and y), t is the index for values of x and y *representing time*, and k is the number of data points over which the cumulative summation is performed.

Next, root-mean square (*RMS*) is computed over each of the non-overlapping subseries v, of different lengths s. Here, the data profile is detrended by a polynomial of the user's choice (y_v). Commonly used trends are linear, exponential, or quadratic. However, higher order detrending fluctuations or adaptive detrending (Riley, Bonnette, Kuznetsov, Wallot, & Gao, 2012) are possible. Note that the higher the order of the polynomial used, the larger the minimum subseries size needs to be to retain variance in the residuals. Moreover, detrending can be done in a more continuous manner, such as using overlapping windows (particularly if the time series is not an integer multiple of the base of the logarithmic function used; so that some part of the time series would otherwise not be represented in the scaling function; Kantelhardt et al., 2002) or smoothly connecting the detrending functions across windows (Riley et al., 2012). These choices depend on the properties of the data at hand. For non-overlapping subseries, the RMS is defined as

$$RMS(v, s) \equiv \frac{1}{s} \sum_{t=1}^{s} \{y[(v-1)s + t] - y_v(t)\}^2, v = 1, \cdots, N_s, \tag{2}$$

where v is the index for the subseries of length s, s is the number of subseries of a certain length, $N_s \equiv \text{int}(N/s)$, and y_v is the value of polynomial fit in subseries v. Then, an aggregated *RMS* value is derived across the same length category of the corresponding subseries s (i.e., the same timescales):

$$RMS(s) \equiv \left\{ \frac{1}{s} \sum_{v=1}^{s} RMS(v, s) \right\}^{\frac{1}{2}}, \tag{3}$$

where *RMS* is root-mean-square fluctuations.

Finally, the Hurst exponent is the estimated slope L of the linear relationship of the logarithm of *RMS* and the logarithm of s, so that $H = L$:

$$RMS(s) \sim s^L, \tag{4}$$

where L is the slope of the regression line, estimating H.

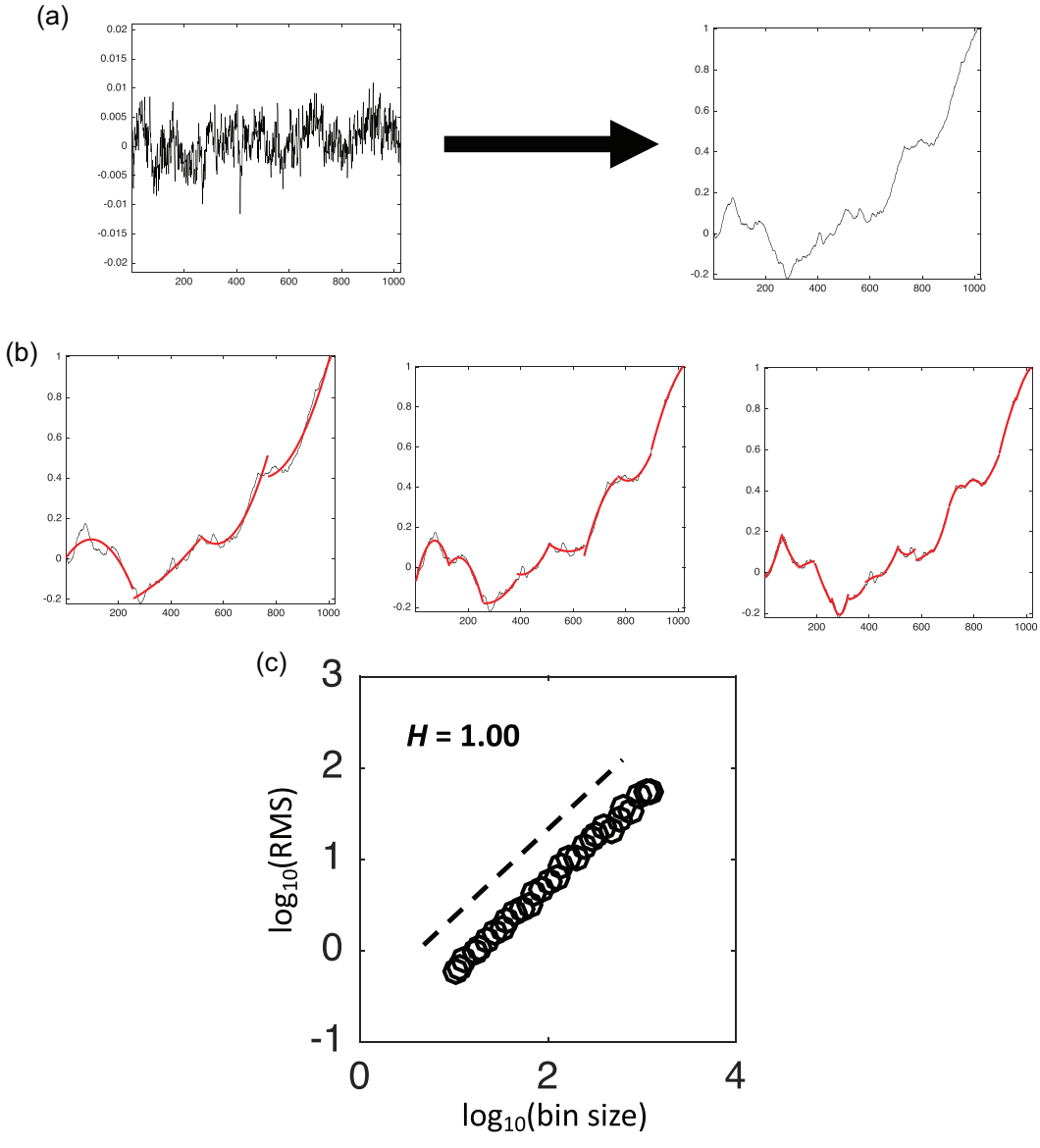

Fig. 1. DFA procedure: (A) The time series is converted into a cumulative profile; (B) the profile is divided into non-overlapping subseries and the local trend is removed—this procedure is then repeated for subseries of different lengths; (C) The logarithm of the subseries length (bin size) is plotted against the logarithm of average variance of the residuals (RMS). The slope of a linear trend line fitted to this plot is an estimate of the Hurst exponent *H*.

To extend the univariate DFA algorithm to a multivariate algorithm, we need to extend the calculation of the variances in Step 2. A multidimensional time series consists of multiple ($D > 1$) dimensions or component time series $y(t) = (y_1(t),\ldots,y_D(t))'$. Hence, for each subsegment as computed in (2), we have multiple variances (the *RMS*′) and covariances, which can be summarized in a variance–covariance matrix C:

$$C = \begin{bmatrix} \mathrm{Var}_{d1(v,s)} & \mathrm{Cov}_{d1,d2(v,s)} & \cdots & \mathrm{Cov}_{d1,dD(v,s)} \\ \mathrm{Cov}_{d2,d1(v,s)} & \mathrm{Var}_{d2(v,s)} & & \mathrm{Cov}_{d2,dD(v,s)} \\ \vdots & & \ddots & \vdots \\ \mathrm{Cov}_{dD,d1(v,s)} & \mathrm{Cov}_{dD,d2(v,s)} & \cdots & \mathrm{Var}_{dD(v,s)} \end{bmatrix}, \tag{5}$$

where d is a dimension (component time series) of the multidimensional time series y_d, D is the number of dimensions (component time series) of the multidimensional time series y_d, Var_d(v,s) is the variance (i.e., *RMS* fluctuation) of subseries v of length s, and $\mathrm{Cov}_{d,d'}$(v,s) is the covariance of the fluctuations for subseries v of length s of the components d and d', with $d,d' = 1, \ldots, D$, with $d \neq d'$.

The different *RMS*′ for the subseries with a length s of a dimension (component time series) d of the original multidimensional time series x can be computed analogously to Eq. 2:

$$Var_d(v,s) = RMS_d(v,s) \equiv \frac{1}{s}\sum_{t=1}^{s}\left\{y_d\left[(v-1)s+t\right] - y_{v,d}(t)\right\}^2,\ v = 1,\cdots,N_s,\ d = 1,\cdots,D, \tag{6}$$

where N_s is the number of subseries of a certain length, $N_s \equiv \mathrm{int}(N/s)$.

The covariances between each pair of subseries with length s of the dimensions d and d' dimensions (with $d,d' = 1, \ldots, D$, and $d \neq d'$) of the original multidimensional time series x can be computed by

$$Cov_{d,d'}(v,s) \equiv \frac{1}{N_s}\sum_{t=1}^{N_s}\left\{y_d\left[(v-1)s+t\right] - y_{v,d}(t)\right\} * \left\{y_{d'}\left[(v-1)s+t\right] - y_{v,d'}(t)\right\},$$

$$v = 1,\cdots,N_s,\ d, d' = 1,\cdots,D, \quad d \neq d'. \tag{7}$$

Now, we propose two ways to determine the average multivariate root-mean-square fluctuations for the different subsequences from Eq. 5, the total variance (RMS_{tot}) or the generalized variance (RMS_{gen}). RMS_{tot} simply involves the sum of the diagonal elements of C, that is, its trace:

$$RMS_{tot}(v,s) \equiv \left\{\frac{1}{N_s}\sum_{v=1}^{N_s}\mathrm{tr}\left(C_{v,s}\right)\right\}^{\frac{1}{2}}, \tag{8}$$

where tr is the trace, C is the variance–covariance matrix of subseries v of length s for the different dimensions of the multidimensional time series y, and N_s is the number of subseries of a certain length, $N_s \equiv \mathrm{int}(N/s)$.

As the total variance approach does not take the covariances of the time series into account, we propose RMS_{gen} as the determinant of the variance–covariance matrix between

the dimensions, which is a measure of linear dependence:

$$RMS_{gen}(v,s) \equiv \left\{ \frac{1}{N_s} \sum_{v=1}^{N_s} \det\left(C_{v,s}\right) \right\}^{\frac{1}{2}}, \tag{9}$$

where det is the determinant.

This results in an adjustment of the global variance by the covariances between the different dimensions of a multivariate time series in a linear manner. It also implies that the fastest timescale that can be investigated (i.e., the smallest subsequence) needs to be greater than D. Otherwise, the generalized variance cannot be calculated as the determinant would always be zero. The fluctuation function and the Hurst exponent based on RMS_{tot} (H_{tot}) can then be computed via Eq. 4: $H_{tot} = L$. While the Hurst exponent based on RMS_{gen} (H_{gen}) is calculated analogously, we subsequently need to adjust it by the number of dimensions of the multivariate time series, so that $H_{gen} = L/D$.

We note that the trace of a covariance matrix is dominated by the largest variance. Consequently, a component with comparably much higher variance may dominate the behavior of the trace across timescales and, therefore, the estimated Hurst exponent. This behavior is comparable to the dependence of the component selection of principal component analysis (PCA), where variables with higher variance result in higher weights. This is why usually the correlation matrix is used as an input for PCA. Similar considerations should apply for the total variance version and a standardized version of the time series might be a good default approach. Then again, if all variables are measured in the same metric, the actual differences in variance—and hence, the differential influence of the individual component time series on the overall result—might be meaningful, such as for the Lorenz system. In any case, this is not an issue with the generalized variance method.

Finally, a practical note on the application of multivariate DFA: As with any multivariate technique, the choice of the set of dependent variables is crucial. Researchers need to have some minimal understanding of which variables can be meaningful. Moreover, consider the case where one assumes that two variables, both measured from one system, show very different Hurst exponents. One shows $H = 0.5$, the other $H = 1.5$. Just by itself, this does not necessarily imply that these two time series should not be analyzed together. For example, if we suspect that the system is poised to stay near a critical state globally and that this is indicated by system-level behavior that shows fluctuations of H around 1.0, but might have to archive this by complementary dynamics spread across the system, then this might be two variables that can be meaningfully analyzed together.

3. Application 1: Test on artificial multidimensional time series with nonlinearly interacting dimensions

In the following section, the mvDFA algorithm will be tested on data generated by the Lorenz system (Lorenz, 1963), which exhibits fractal scaling properties (Yang & Zheng, 2010). The Lorenz system is an ordinary differential equation system and consists of the

Table 1
Average Hurst exponents, standard deviations, and confidence intervals of the Lorenz system obtained from univariate and multivariate DFA

Method	Mean H	$SD\ H$	Lower Bound of 95% Confidence Interval	Upper Bound of 95% Confidence Interval
H_{tot}	0.900	0.015	0.870	0.931
H_{gen}	0.822	0.004	0.813	0.832
H_{uni}	0.910	0.007	0.896	0.922
H_{x_uni}	1.008	0.016	0.976	1.040
H_{y_uni}	0.926	0.016	0.893	0.958
H_{z_uni}	0.650	0.22	0.608	0.691

Note. The estimates were obtained from 1,000 simulations of the Lorenz system. H_{tot} is the total variance mvDFA, H_{gen} is the generalized variance mvDFA, H_{uni} is an averaged univariate DFA. $H_{x\text{-}uni}$, $H_{y\text{-}uni}$, and $H_{z\text{-}uni}$ are the univariate DFA exponents computed separately for the three dimensions of the Lorenz system. The confidence intervals are related to the individual distributions and do not reflect differences between the methods.

following three equations (Eq. 10):

$$\frac{dx}{dt} = \sigma \cdot (y - x),$$

$$\frac{dy}{dt} = x \cdot (\rho - z) - y,$$

$$\frac{dz}{dt} = x \cdot y - \beta \cdot z. \tag{10}$$

In order to test the mvDFA algorithms, we ran 1,000 simulations using the parameter values of $s = 10$, $s = 28$, and $b = 8/3$, and initial starting values of $x = y = z = 0.1 + e$, where e was drawn from a uniform distribution, $U[-0.1, 0.1]$ for each run and parameter. Within these parameter settings, the Lorenz attractor stays in the chaotic regime of a strange attractor. In this manner, 100k data points were simulated in each run, each yielding a separate instantiation of the Lorenz system dynamics, on which mvDFA was performed. We used both multivariate extensions, RMS_{tot} and RMS_{gen}, but also applied the univariate DFA algorithm for each dimension separately and subsequently averaged across the three dimensions.

The resulting three calculations of the Hurst exponent, H_{uni} (i.e., univariate averaged), H_{tot}, and H_{gen} were compared on the average fit of the linear scaling function (R^2), and the resulting estimated Hurst exponents H for the behavior of the three-dimensional system. The parameters used for all analyses were a minimum bin size of 200, a maximum bin size of 1/8 of the size of the time series, and trends removed up to quadratic. Inferential statistics were conducted as paired-sample t-tests with stats-package in R. The results are summarized in Table 1.

The following is apparent from Table 1: First, when examining the different dimensions of the Lorenz system univariately, the resulting Hurst exponents differ substantially. They do not converge to a single value that characterizes the system's dynamics. Second, their

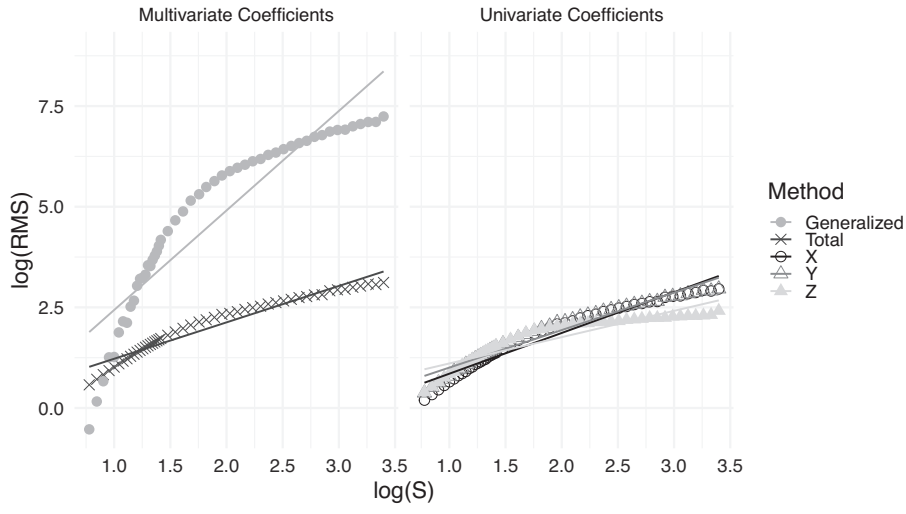

Fig. 2. Example scaling functions for the different methods. The left panel displays the results from the multivariate analyses, and the right panel displays the results from the univariate analyses. All methods reveal multiscale fluctuations with a break point between 1.5 and 2.0 log(s). This is most pronounced for the generalized variance approach.

average differs from the multivariate estimates, which is corroborated by central averages and confidence intervals in Table 1, where H_{uni} is larger than H_{tot}, which in turn is larger than H_{gen}. When investigating the fit of the scaling function, the average univariate method yields an $R^2{}_{uni} = 0.910$ ($SD = 0.007$), the total variance method yields an $R^2{}_{tot} = 0.942$ ($SD = 0.006$), and the generalized variance method results in $R^2{}_{gen} = 0.847$ ($SD = 0.012$).

In sum, the individual dimensions do not converge on the same estimates for H, and their average is different to the multivariate approaches. However, all approaches do classify the fluctuations of the Lorenz system to be persistent. While the total variance method also exhibits a better fit for the scaling function, this is not the case for the generalized variance method. Moreover, the fit for the scaling function of the generalized variance method is worse than the average of the univariate analyses. One reason for this could be that the relations among the dimensions of the Lorenz system are highly non-linear so that the linear approximation of these correlations inherent in the generalized variance methods biases the results.

However, another reason becomes apparent when investigating the scaling functions visually (Fig. 2). There is a scale break in the scaling function between 1.5 and 2.0 log(s), most pronounced for the generalized variance method. This could be due to different behavior of the Lorenz system at different scales or simply a function of accuracy of the numerical integration of the system. The latter leads to highly correlated data points on the fast timescales, in which fluctuations are not very reflective of the dynamics of the system. If we only fit the scaling function to bin sizes log(s) > 1.5, the fits improve to $R^2{}_{uni} = 0.952$, $R^2{}_{gen} = 0.950$, and $R^2{}_{tot} = 0.984$. If we only consider log(s) > 2.0, the fits improve even more to $R^2{}_{uni} = 0.980$,

$R^2_{gen} = 0.990$, and $R^2_{tot} = 0.993$. Under these conditions, the generalized variance method also exhibits a better fit than the univariate approach, albeit by a slim margin.

Another interesting test to compare the two methods is how they capture a change of behavior in the system. For example, Stephen, Boncoddo, Magnuson, and Dixon (2009) provided a moving-window analysis for the Lorenz system going through a phase transition from a homoclinic orbit to strange attractor dynamics. Here, they showed that the change in fractal exponents indicates when the system leaves one phase into the phase transition and finally settling into the new phase. Here, we used each of the individual dimensions of the Lorenz system to conduct such an analysis as well as the multivariate total and generalized variance methods. Fig. 3 shows that the exponents from the univariate analyses fluctuate a lot, while the total variance method provides a somewhat better distinction between the two phases. However, only with the generalized variance method do we see a high stability of the scaling exponents within each phase on the one hand and a clear change in scaling exponents at the phase transition on the other hand.

4. Application 2: Test on 64-channel EEG during time estimation

A common source of multivariate time series is neurophysiological recordings, for example, EEG or functional magnetic resonance imaging. In this section, we present data of a time estimation task with continuous EEG recordings. Based on this dataset, we will further test the mvDFA algorithms. Moreover, we outline how mvDFA can be used to evaluate hypotheses about global changes in fractal dynamics of multivariate time series as well as interactions between neurophysiology and behavior considering the question of control organisms.

While conventionally, control in humans is thought to flow from neurophysiological processes to behavior, it is discussed as a matter of timescales in complex systems theory and SOC: Observing power-law behavior in human data that show persistent fluctuations has led to the proposal that processes on slower timescales usually constrain processes on faster timescales (Van Orden, Hollis, & Wallot, 2012). However, what follows from this conjecture is not quite clear for the question of control between neurophysiological and behavioral processes because both, behavioral and neurophysiological data, exhibit fractal fluctuations over time (e.g., Goldberger et al., 2002; He, 2011; Holden et al., 2011; Kuznetsov & Wallot, 2011; Lutzenberger, Elbert, Birbaumer, Ray, & Schupp, 1992). In other words, both contain systematic patterns of variation on longer timescales disguising which of the two resides on slower timescales, hence, constraining the other more strongly.

Here, the hypothesis has been extended (Van Orden, 2010; Van Orden et al., 2011, 2012) to contain (mutual) constraints between physiological and behavioral processes that are contingent on temporal regularities in behavioral (and by extension social and environmental) processes. That is, while neurophysiological processes control behavior, they are themselves co-controlled by the temporal regularities of the behavioral processes that they cause. This also suggests a pathway for the emergence of scales in otherwise scale-free processes, such as neurophysiological processes captured in EEG recordings. Behavioral regularities (which

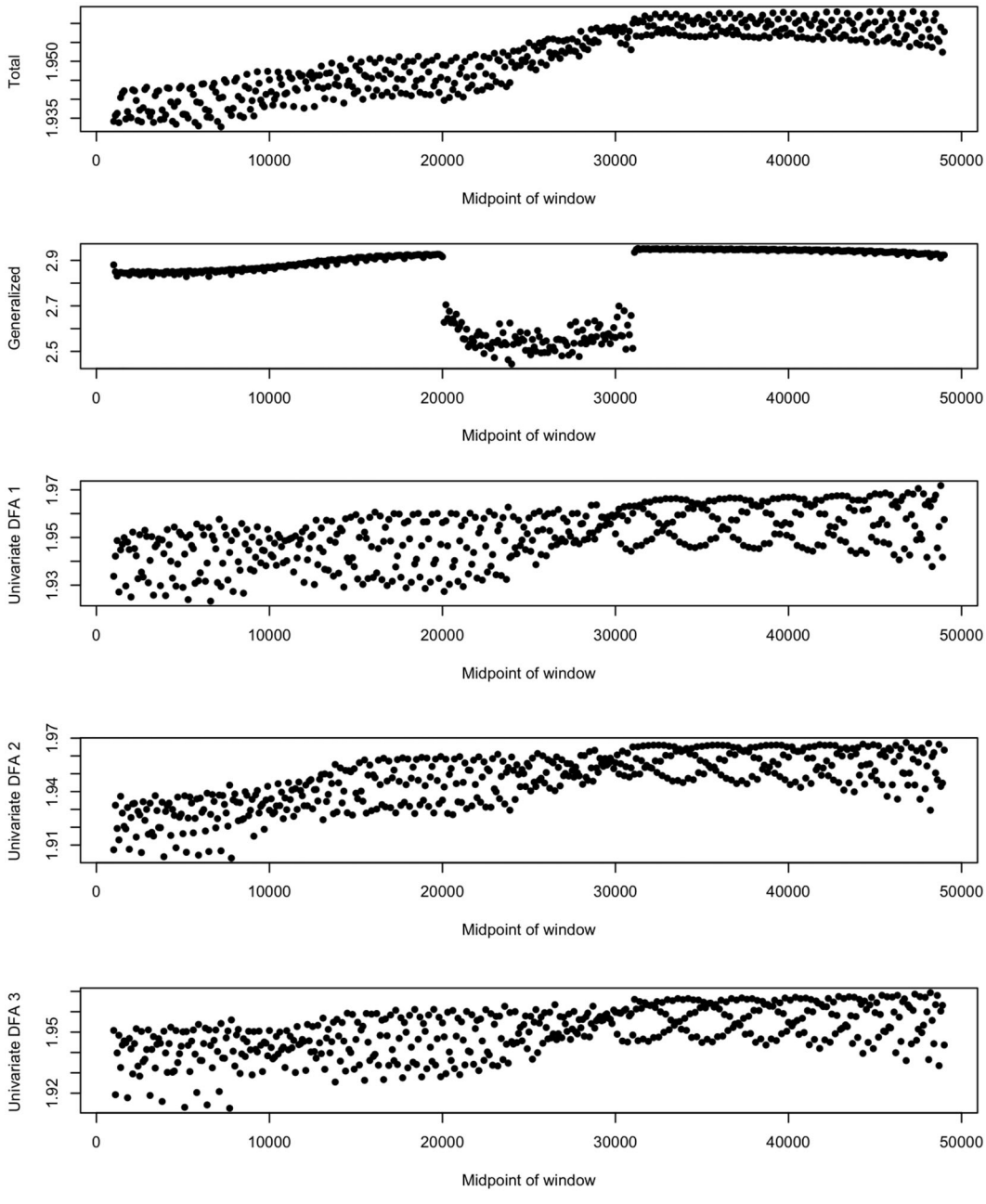

Fig. 3. The Lorenz system going through a phase transition (middle 20% of the data) from a homoclinic orbit (first 40% of the data; parameter settings: $s = 10$, $s = 28$, and $b = 8/3$) to strange attractor (last 40% of the data; parameter settings: $s = 15$, $s = 25$, and $b = 3.5$). The univariate analysis (bottom three rows), but also the total variance method (top panel), shows very variable coefficients. The generalized variance method (second panel) provides the clearest picture of the transition process.

are themselves contingent on task properties) introduce temporarily preferred scales into neurophysiological processes.

To investigate this proposal, we conducted a timing study similar to Kuznetsov and Wallot (2011), who had participants perform a simple time-estimation task by pressing a response key every time they thought a second had passed. Participants either received visual feedback about their performance or not. The introduction of feedback did not change the standard deviation of time interval estimates, but DFA revealed a change in long-range correlations of the time interval estimates. The introduction of feedback significantly reduced the degree of long-range correlation in participants' time interval estimation performance. This suggested an increased coupling between motor-cognitive timing processes and environmental regularities (Kuznetsov & Wallot, 2011; Van Orden, 2010).

In the current study, 10 participants (students and faculty from Aarhus University) were presented with auditory stimuli at 10 one-second time intervals and then asked to consecutively press a key at that interval for 1,100 times. Here, participants saw the number "1" in a circle on a screen to remind the participants to keep pressing the key at 1-s intervals. Every time they pressed the response key, the circle flickered briefly to indicate that the response had been recorded.

In the feedback condition, participants were provided with visual feedback after each tap, indicating how much they deviated from the target interval (in milliseconds). Here, participants also saw the number "1" in a circle on a screen to remind the participants to keep pressing the key at 1-s intervals. Additionally, after having pressed the button, participants saw a message about their performance for 400 ms below the circle. If they pressed the button *X* milliseconds too early, the message read "X ms early." If they pressed the button *X* milliseconds too late, the message read "X ms late." In the no-feedback condition, no such feedback was provided, of course. The order in which the conditions were presented was randomized between participants.

The study was evaluated and received an ethics waiver from the ethics committee of the Central Denmark Region and was conducted in accordance with the Declaration of Helsinki. Written consent was obtained from all participants.

EEG was collected with 64 active Ag/AgCl electrodes that were arranged according to the international 10–20 system in an elastic electrode cap. Two electrodes (sites PO9 and PO10) were applied next to and below the left eye to monitor eye movements and blinks. The ground electrode was placed at site AFz, and FCz was used as the online reference electrode. The signal was amplified with an actiCHamp amplifier and continuously recorded with the BrainVision Recorder software (BrainProducts GmbH). Data were sampled at 1 kHz with an online 0.1 Hz high-pass filter. No offline filter was applied to the data. Based on the electrooculogram, an automatic artifact rejection was carried out with a cutoff value of 150 μV. EEG data were then downsampled to 250 Hz to reduce computation time. Furthermore, the time series were standardized to distribute weights evenly to all components for the generalized and total variance methods. Subsequently, we conducted averaged univariate DFA, total-variance mvDFA, and generalized-variance mvDFA on the pre-processed μV-time series. For averaged univariate DFA, the μV-time series for each electrode was subjected to standard univariate DFA, and then coefficients were averaged over all electrodes. For the multivariate

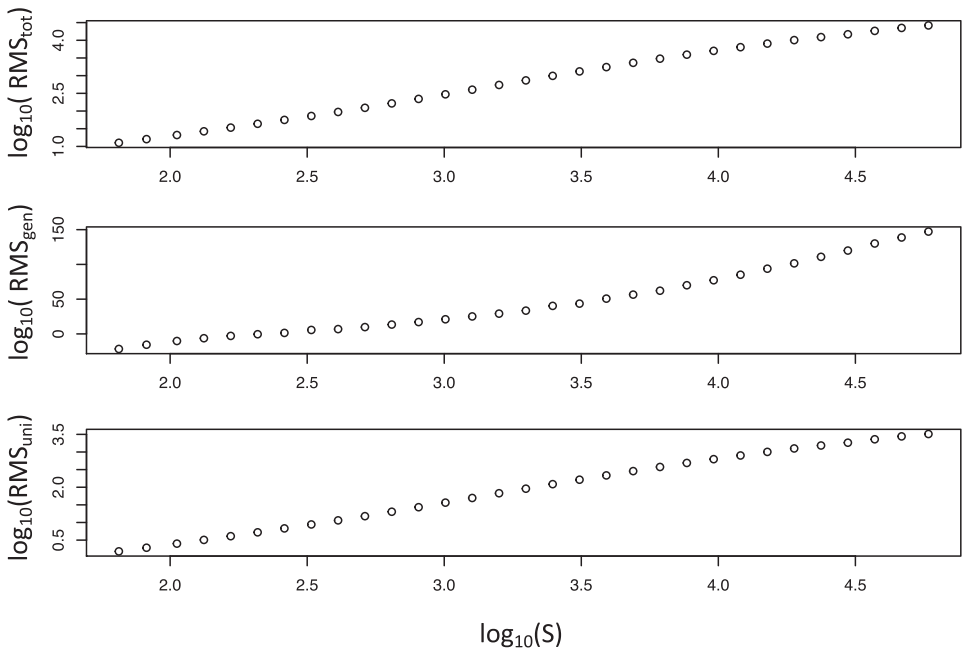

Fig. 4. Depiction of the average fluctuation function for total variance mvDFA (RMS_{tot}), generalized variance mvDFA (RMS_{gen}), and averaged univariate DFA (RMS_{uni}).

methods, μV-time series for all electrodes entered the analysis simultaneously. The calculation of the respective Hurst exponents was performed separately over the whole approximate 20-minute EEG recordings in the feedback and no-feedback conditions for each participant, respectively.

We expected to find a break in the scale-free, fractal fluctuations of the EEG data around 1 Hz due to participants pressing a response key approximately every second during the time-estimation task. This should then translate into a change in scaling relations for fractal fluctuations below and above bin sizes of 250 data points. Fig. 4 shows the average fluctuation functions across conditions and participants for the three types of mvDFA. It seems that multiscale fluctuations around $\log_{10}(s) = 2.4$ (i.e., a subseries length of 250 data points) are most visible for the generalized variance method.

To validate the visual impression, we ran two types of mixed-linear models on the fluctuation function data for each method, participant, and trial, with RMS_{uni}, RMS_{tot}, and $\mathrm{RMS}_{\mathrm{gen}}$ as dependent variables, respectively. The first model only incorporated $\log_{10}(s)$ as the predictor, thus, modeling the assumption that there is only one homogenous scale-free process:

$$\log10(RMS_{i,j}) = \gamma_{00} + \gamma_{01}\log10\,(s) + u_{0j} + e_{i,j}, \quad \text{(M1)}$$

where $\log_{10}(RMS_{i,j})$ is a dependent variable containing the logarithmized average RMS fluctuations at specific subseries lengths s, γ_{00} is a fixed intercept, γ_{10} is the fixed slope for

Table 2
Model comparison for including the predictor $\log_{10}(s)$SLOW into fitting the fluctuation function for averaged univariate, total, and generalized variance DFA

DV	ΔAIC	ΔBIC	χ^2	*df*	*p*
RMS_{uni}	−0.6	−3.9	2.55	1	.110
RMS_{tot}	−0.1	−4.4	1.98	1	.159
RMS_{gen}	−217.5	−213.1	219.54	1	<.001

Note. DV: dependent variable; DAIC: difference in Akaike's information criterion (M2 – M1); DBIC: difference in Bayesian information criterion (M2 – M1).

predictor $\log_{10}(s)$, $\log_{10}(s)$ is a predictor variable containing logarimized subseries lengths s, u_{0j} is a random intercept for participants, $e_{i,j}$ is residual, i is an index for RMS fluctuations at a specific subseries length within participants, and j is an index for participants.

The second model included an additional predictor $\log_{10}(s)$SLOW, which captures deviations from the overall scaling function for the slower fluctuations (i.e., bigger bin sizes) larger than 1 second:

$$\log10(RMS_{i,j}) = \gamma_{00} + \gamma_{01}\log10\,(s) + \gamma_{02}\log10\,(s)\,\mathrm{SLOW} + u_{0j} + e_{i,j} \quad \text{(M2)}$$

where γ_{02} is the fixed slope for a predictor and log10(s)SLOW is a predictor variable containing logarimized subseries lengths s for $s > 250$ data points (i.e., fluctuations bigger than 1 second).

Model comparison between (M1) and (M2) for RMS_{uni}, RMS_{tot}, and RMS_{gen} revealed a significant contribution for adding the predictor $\log_{10}(s)$SLOW to the model if the fluctuation function is based on the generalized variance method (see Table 2). That is, the model provides evidence for a scale-break around 1 second, if we take the correlations among the multivariate EEG data into account. However, no break is suggested by the data if we treat them as independent.

Accordingly, we found evidence for the hypothesis that behavioral and neurophysiological processes interact: One interpretation is that one set of processes (here behavioral) changed the fractal scaling so that we see the emergence of a dominant scale in the neurophysiological data. The results suggest that control can flow from behavior to neurophysiology in that environmental regularities (feedback) constrain behavioral regularities (button pressing behavior) which, by virtue of proprioception, constrain timing-related processes in the nervous system. However, we only find this pattern of results using the generalized variance mvDFA. Note that we also ran a model including interactions with condition (i.e., feedback vs. no feedback), but feedback did not moderate the effect of multivariate scaling. Furthermore, there is a moderate degree of variability in the Hurst exponents across the 62 univariate analyses for each channel: The average standard deviation (within each participant) of H was 0.08 (for both, the condition with, and without feedback).

5. Conclusion

In this paper, we addressed a question that has both a theoretical and a methodological aspect. Our starting point was the strong view of interaction-dominant dynamics in which in a system that runs on SOC; each component reflects the whole system dynamics. The consequence would be that there is little need to measure multiple parts of a system. We demonstrated how univariate DFA, which is a key technique to capture traces of SOC in human data, can be extended to multivariate DFA. For a model system, the Lorenz attractor, we demonstrated the application of mvDFA, and how multivariate methods improve the analysis of such systems over univariate approaches. Based on EEG data, we showed how mvDFA (i.e., the generalized variance method) uncovers results that cannot be observed with a univariate approach. Because the total variance method treats the different component time series as independent, it yielded similar results to the averaged univariate analysis.

Further developments of these methods need to consider the potentially complex relationship between the component time series of one system. If the system is interaction dominant, and the interactions within the system are nonlinear (as suggested by observed multifractal fluctuations in human data; e.g., Kelty-Stephen & Mangalam, 2022), then the assumption of linearity in the relations between the component time series inherent in the generalized variance approach can only be seen as a first approximation. Ideally, it needs to be replaced by model-free correlation techniques or proper (nonlinear) correlation functions. This, however, requires substantial knowledge of the phenomena at hand.

Theoretically, our results suggest that the strong version of the interaction-dominant interpretation of SOC in human organisms does not hold. Regarding the human mind and body, the results of our EEG data suggested that the dynamics of one component do not reflect the system as a whole. In our view, however, this result does by no means undermine the notion of interaction-dominant dynamics, or SOC as a driving force in the organization of organisms. It rather points to the need to refine such theorizing and to consider the necessity of more encompassing, multivariate measures of complex systems to understand them. The multivariate extension of DFA presented here might be one tool to conduct such research because the notion of "system" carries with it the understanding that something consists of multiple parts. From the perspective of dynamic systems, it is of interest to better understand how these parts interact and lead to global, coordinated behavior.

Acknowledgments

SW acknowledges funding from the German Science Foundation (DFG; Heisenberg programme, funding ID: 442405852). The project acknowledges funding from the Danish National Research Foundation's grant to CFIN and the MINDLab grant from the Danish Ministry of Science, Technology and Innovation.

Open access funding enabled and organized by Projekt DEAL.

References

Bak, P. (1996). *How nature works: The science of self-organized criticality*. Berlin, Germany: Springer.

Bronfenbrenner, U. (1976). *Ökologische Sozialisationsforschung*. Stuttgart, Germany: Klett.

Brown, C. T., & Liebovitch, L. S. (2010). *Fractal analysis*. Quantitative Applications in the Social Sciences (Vol. 165). Thousand Oaks, CA: SAGE.

Favela, L. H. (2020). Dynamical systems theory in cognitive science and neuroscience. *Philosophy Compass*, *15*(8), e12695, https://doi.org/10.1111/phc3.12695

Gilden, D. L., Thornton, T., & Mallon, M. (1995). 1/f noise in human cognition. *Science*, *267*, 1837–1839.

Goldberger, A. L., Amaral, L. A., Hausdorff, J. M., Ivanov, P. C., Peng, C. K., & Stanley, H. E. (2002). Fractal dynamics in physiology: Alterations with disease and aging. *Proceedings of the National Academy of Sciences*, *99*, 2466–2472.

He, B. J. (2011). Scale-free properties of the functional magnetic resonance imaging signal during rest and task. *Journal of Neuroscience*, *31*, 13786–13795.

Holden, J. G. (2005). Gauging the fractal dimension of response times from cognitive tasks. In M. A. Riley & G. Van Orden (Eds.), *Tutorials in contemporary nonlinear methods for the behavioral sciences* (pp. 267–318). Washington, DC: National Science Foundation. https://www.nsf.gov/pubs/2005/nsf05057/nmbs/nmbs.pdf

Holden, J. G., Choi, I., Amazeen, P. G., & Van Orden, G. (2011). Fractal 1/*f* dynamics suggest entanglement of measurement and human performance. *Journal of Experimental Psychology: Human Perception and Performance*, *37*, 935–948.

Irmer, J. P., & Wallot, S. (2023). mvDFA: Multivariate detrended fluctuation analysis. R package version 0.0.4. https://CRAN.R-project.org/package=mvDFA

Jensen, H. J. (1998). *Self-organized criticality*. Cambridge, England: Cambridge University Press. https://doi.org/10.1017/CBO9780511622717

Kantelhardt, J. W., Zschiegner, S. A., Koscielny-Bunde, E., Havlin, S., Bunde, A., & Stanley, H. E. (2002). Multifractal detrended fluctuation analysis of nonstationary time-series. *Physica A: Statistical Mechanics and Its Applications*, *316*(1-4), 87–114.

Kello, C. T., Brown, G. D., Ferrer-i-Cancho, R., Holden, J. G., Linkenkaer-Hansen, K., Rhodes, T., & Van Orden, G. C. (2010). Scaling laws in cognitive sciences. *Trends in Cognitive Sciences*, *14*(5), 223–232.

Kelty-Stephen, D. G., & Mangalam, M. (2022). Fractal and multifractal descriptors restore ergodicity broken by non-Gaussianity in time-series. *Chaos, Solitons & Fractals*, *163*, 112568.

Kelty-Stephen, D. G., & Wallot, S. (2017). Multifractality versus (mono-) fractality as evidence of nonlinear interactions across timescales: Disentangling the belief in nonlinearity from the diagnosis of nonlinearity in empirical data. *Ecological Psychology*, *29*(4), 259–299.

Köhler, W. (1940). *Dynamics in psychology*. Now York, NY: Liveright.

Kuznetsov, N. A., & Wallot, S. (2011). Effects of accuracy feedback on fractal characteristics of time-estimation. *Frontiers in Integrative Neuroscience*, *5*, 62.

Lewin, K. (1939). Field theory and experiment in social psychology. *American Journal of Social Psychology*, *44*, 868–896.

Lorenz, E. N. (1963). Deterministic nonperiodic flow. *Journal of Atmospheric Sciences*, *20*(2), 130–141.

Lutzenberger, W., Elbert, T., Birbaumer, N., Ray, W. J., & Schupp, H. (1992). The scalp distribution of the fractal dimension of the EEG and its variation with mental tasks. *Brain Topography*, *5*(1), 27–34.

Mandelbrot, B. (1997). *Fractals and scaling in finance*. New York, NY: Springer. https://doi.org/10.1007/978-1-4757-2763-0

Peng, C. K., Havlin, S., Stanley, H. E., & Goldberger, A. L. (1995). Quantification of scaling exponents and crossover phenomena in nonstationary heartbeat time-series. *Chaos*, *5*, 82–87.

R Core Team. (2022). R: A language and environment for statistical computing. Vienna, Austria: R Foundation for Statistical Computing. https://www.R-project.org/.

Riley, M. A., Bonnette, S., Kuznetsov, N., Wallot, S., & Gao, J. (2012). A tutorial introduction to adaptive fractal analysis. *Frontiers in Physiology*, *3*, 371.

Simon, H. A. (1973). The organization of complex systems. In H. H. Pattee (Ed.), *Hierarchy theory: The challenge of complex systems* (pp. 1–27). New York, NY: George Braziller.

Stephen, D. G., Boncoddo, R. A., Magnuson, J. S., & Dixon, J. A. (2009). The dynamics of insight: Mathematical discovery as a phase transition. *Memory & Cognition*, *37*, 1132–1149.

Sternberg, S. (1969). The discovery of processing stages: Extensions of Donders' method. *Acta Psychologica*, *30*, 276–315.

van Gelder, T. (1998). The dynamical hypothesis in cognitive science. *Behavioral and Brain Sciences*, *21*(5), 615–628. https://doi.org/10.1017/S0140525x98001733

Van Orden, G. (2010). Voluntary performance. *Medicina*, *46*(9), 581.

Van Orden, G., Holden, J. G., & Turvey, M. T. (2003). Self-organization of cognitive performance. *Journal of Experimental Psychology: General*, *132*(3), 331–350.

Van Orden, G., Holden, J. G., & Turvey, M. T. (2005). Human cognition and 1/*f* scaling. *Journal of Experimental Psychology: General*, *134*(1), 117.

Van Orden, G., Hollis, G., & Wallot, S. (2012). The blue-collar brain. *Frontiers in Physiology*, *3*, 207.

Van Orden, G. C., & Kloos, H. (2003). The Module Mistake. *Cortex*, *39*(1), 164–166. https://doi.org/10.1016/s0010-9452(08)70092-3

Van Orden, G., Kloos, H., & Wallot, S. (2011). Living in the pink: Intentionality, well-being, and complexity. In C. Hooker (Ed.), *Philosophy of complex systems* (pp. 629–672). Amsterdam, The Netherlands; North-Holland.

Van Orden, G. C., Pennington, B. F., & Stone, G. O. (2001). What do double dissociations prove? *Cognitive Science*, *25*, 111–172.

Wagenmakers, E.-J., Farrell, S., & Ratcliff, R. (2004). Estimation and interpretation of 1/*f* noise in human cognition. *Psychonomic Bulletin & Review*, *11*, 579–615.

Wagenmakers, E.-J., Farrell, S., & Ratcliff, R. (2005). Human cognition and a pile of sand: A discussion on serial correlations and self-organized criticality. *Journal of Experimental Psychology: General*, *134*(1), 108–116.

Wallot, S., & Kelty-Stephen, D. G. (2018). Interaction-dominant causation in mind and brain, and its implication for questions of generalization and replication. *Minds and Machines*, *28*(2), 353–374.

Xiong, H., & Shang, P. (2017). Detrended fluctuation analysis of multivariate time-series. *Communications in Nonlinear Science and Numerical Simulation*, *42*, 12–21.

Yang, Q., & Zeng, C. (2010). Chaos in fractional conjugate Lorenz system and its scaling attractors. *Communications in Nonlinear Science and Numerical Simulation*, *15*(12), 4041–4051.